

Reactive Transport Modeling to Support Long-Term Monitoring Strategy: Ion Exchange Induced Contaminant Remobilization at Subsurface Contaminated Sites Influenced by Abrupt Changes in Geochemical Conditions

Sol-Chan Han^{,a,1}, Hansell Gonzalez-Raymat^b, Miles Denham^c, Toshiyuki Bandai^a, Zexuan Xu^a,
Sergi Molins^a, Haruko Wainwright^{*,a,d}*

^aEarth and Environmental Sciences Area, Lawrence Berkeley National Laboratory, 1 Cyclotron Road, Berkeley, CA 94720, USA

^bSavannah River National Laboratory, Savannah River Site, Aiken, 29808, SC, USA

^cPanoramic Environmental Consulting, LLC, P.O. Box 906, Aiken, 29802, SC, USA

^dDepartment of Nuclear Science and Engineering, Massachusetts Institute of Technology, 77 Massachusetts Avenue, Cambridge, MA 02139, USA

***Corresponding authors:**

Sol-Chan Han (schan91@tamu.edu) and Haruko Wainwright (hmwainw@mit.edu)

Present address:

¹Center for Nuclear Security Science and Policy Initiatives, Texas A&M Engineering Experiment Station, College Station, TX 77843, USA

Preprint Status Statement

23 This manuscript is a non-peer-reviewed preprint submitted to EarthArXiv.

24 The manuscript is currently under peer review at the Journal of Contaminant Hydrology.

25 The content of this preprint may differ from the final published version.

26 **ABSTRACT**

27 This study presents a long-term monitoring strategy for early risk warning of the remobilization
28 of contaminants, mainly attenuated through an ion exchange reaction, induced by abrupt changes
29 in geochemical conditions. The strategy aims to utilize readily *in-situ* measurable groundwater
30 quality parameters in the prediction of near-future contaminant remobilization caused by cation
31 exchange reactions. The proposed approach was demonstrated using historical monitoring data
32 from the Department of Energy (DOE) Savanna River Site (SRS) F Area, which experienced
33 abrupt geochemical disturbance during the pump-treat-reinjection remedy, and a reactive transport
34 model developed through this study to understand ^{90}Sr migration behavior in the subsurface of the
35 SRS F Area. The historical monitoring data analysis and reactive transport modeling results
36 suggested that *in-situ* specific conductance sensors can be used for an early warning system to
37 detect contaminant remobilization associated with cation exchange species. This strategy is
38 expected to benefit the long-term management of the contaminated site for elements with cation
39 exchange reactions by providing the means to detect the remobilization of contaminants before the
40 remobilization occurs.

41

42 **KEYWORDS**

43 *Early warning, Long-term monitoring, Contaminated sites, Reactive transport modeling,*
44 *Strontium, Specific conductance*

45

46 **HIGHLIGHTS**

47

- The mechanism of ^{90}Sr remobilization at the Savannah River Site F Area was examined.

48

- A time lag was observed between increases in background electrolyte and ^{90}Sr levels

49

- Increased Na^+ concentrations may induce ^{90}Sr remobilization through ion exchange.

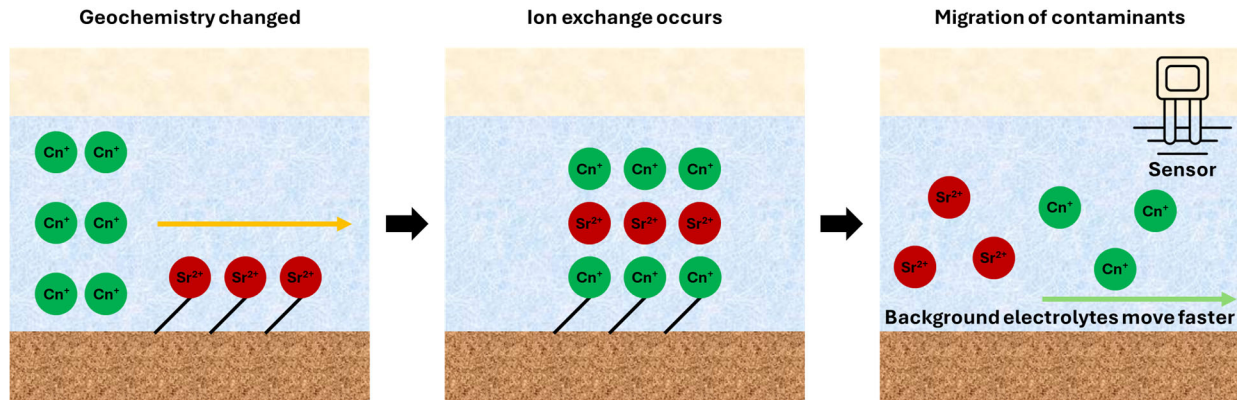
50

- Specific conductance sensor could be used for early detection of ^{90}Sr remobilization.

51

52 GRAPHICAL ABSTRACT

53



54 **1. INTRODUCTION**

55 Increased anthropogenic activities, including rapid industrialization and urbanization, have left
56 subsurface-contaminated sites across the world.¹ It is estimated that there are more than 5 million
57 of contaminated sites globally, which require remediation and redevelopment to ensure future
58 sustainable land use.¹⁻³ Common contaminants found at these sites include persistent organic
59 pollutants, heavy metals, petroleum hydrocarbons, pesticides, chlorinated solvents, inorganics, and
60 radionuclides.⁴ However, less than 10% of potentially contaminated sites worldwide have been
61 remediated even though site contamination has been recognized already in 1960s.⁴ Particularly in
62 the United States, 1340 sites are listed on the National Priorities List (NPL), which classifies sites
63 that warrant cleanup, but remediation goals have been achieved at only 458 sites as of October 01,
64 2024.⁵

65 Recent demand and emphasis on sustainable remediation have generated interest in attenuation-
66 based remediation strategies, such as monitored natural attenuation (MNA) and enhanced natural
67 attenuation (ENA), leveraging variety of attenuation processes to immobilize and/or degrade
68 contaminants.⁶ Natural attenuation processes occurring in the (sub)surface systems include: (1)
69 partitioning via sorption, accumulation, and volatilization; (2) dispersion and dilution; and (3)
70 abiotic and biotic reactions, degradations, and transformations.⁷ Such attenuation-based remedies
71 have been considered cost-effective, less energy-intensive, less intrusive and more sustainable
72 solutions, and are particularly effective for sites where a large volume of soil and groundwater are
73 contaminated with relatively low concentrations and therefore active treatment is no longer
74 feasible.⁸ However, attenuation-based remedies inherently accompany a level of uncertainty in
75 assuring remediation performance and regulatory compliance.

76 At sites where attenuation-based remedies have been deployed, the attenuated contaminants (e.g.,
77 metals and radionuclides) may remain in the subsurface for an extended period. However, changes
78 in site conditions (e.g., hydrology and geochemistry) can impact the effectiveness of the
79 remediation and could potentially remobilize some of the attenuated contaminants.⁹ In particular,
80 the effect of climate change, such as flooding and groundwater level fluctuations, has become an
81 important and emerging topic at contaminated sites (e.g., Libera, et al. 2019;¹⁰ Cavelan, et al.
82 2022;¹¹ Crawford, et al. 2022;¹² Xu, et al. 2022;¹³ Hill et al., 2023;¹⁴). A recent study by Hill et al.,
83 2023 has found that sea level rise would cause groundwater levels to increase, inundating a
84 significant number of coastal contaminated sites in the U.S.¹⁴ The study also warn that an increase
85 in groundwater elevation by only a few centimeters can mobilize soil contaminants and create new
86 exposure pathways, and pumping to prevent floods is expected to elevate the saltwater interface,
87 changing groundwater ionic strength and mobilizing contaminants in soil.¹⁴ Therefore, the sites,
88 where attenuation-based remedies are deployed, often require long-term institutional control and
89 performance monitoring^{9, 15, 16} and entail a burden on demonstrating that the contaminants are
90 persistently attenuated and/or immobilized.

91 Recently, numerous monitoring strategies and technologies have emerged for contaminated site
92 applications, yielding considerable progress in the cost-effectiveness of monitoring system
93 operations and facilitating real-time *in-situ* sensing. For example, a machine learning approach
94 was implemented to monitor sensor location optimization, monitoring well data analysis, and
95 contaminant concentration estimation.^{16, 17} Denham et al. (2020) proposed a new long-term
96 monitoring concept that focuses on measuring the geochemical and hydrological parameters that
97 control the attenuation and remobilization of contaminants while de-emphasizing direct
98 measurement of contaminant concentration.⁹ The benefits of the proposed method include
99 reducing the cumulative cost of long-term monitoring activities and the early detection of changes

100 in environmental conditions. Schmidt et al. (2018) developed an *in-situ* monitoring technique
101 combined with principal component analysis (PCA) and a Kalman filter to continuously estimate
102 the contaminant concentration based on water quality variables, i.e., specific conductance and pH.⁸
103 This technique enables continuous and real-time estimation of contaminants concentration and
104 cost reduction by decreasing the frequency of contaminant sampling.

105 Although recent efforts might significantly improve the long-term monitoring strategy in terms
106 of cost-effectiveness and indirect estimation of contaminant concentrations,^{8, 16} these approaches
107 are based on site-specific correlations and relationships without physical and predictive
108 understanding. It still emphasizes the estimation of the current status of contaminants without
109 addressing potential time lags between *in-situ* measurable parameters and contaminant
110 concentrations. Furthermore, existing techniques, which rely primarily on measuring contaminant
111 concentration, can only provide alerts once the remobilization has occurred.⁹ To the best of the
112 authors' knowledge, however, how monitoring data could be used for early risk warning of
113 contaminant remobilization has not been investigated extensively.

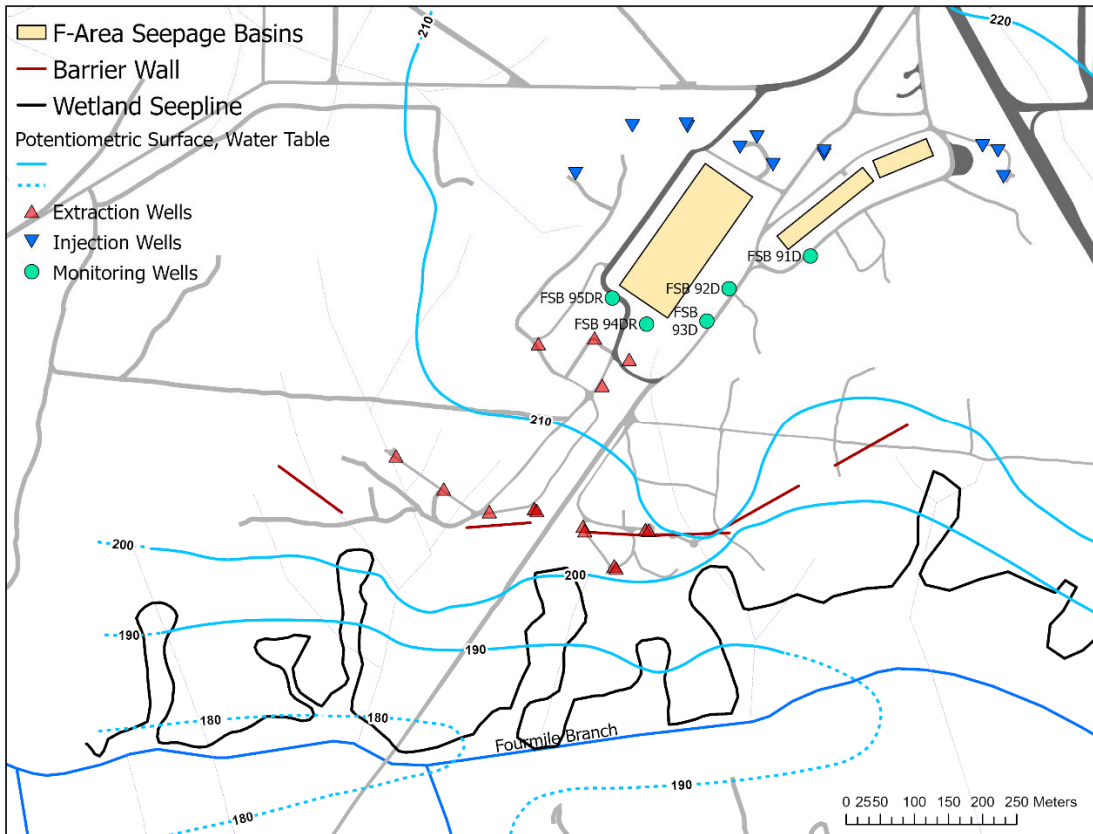
114 To address the current technical gap, this study aims to demonstrate a monitoring strategy for
115 enabling an early warning of contaminant remobilization induced by abrupt changes in
116 geochemical conditions, utilizing *in-situ* measurable variables combined with reactive transport
117 modeling. A particular focus is placed on employing real-time *in-situ* parameters readily
118 measurable by sensors to predict near-future contaminant remobilization caused by cation
119 exchange reactions. We demonstrate this proposed approach using historical monitoring data from
120 the Department of Energy (DOE) Savannah River Site (SRS) F Area, which experienced an abrupt
121 geochemical disturbance due to the pump-treat-reinjection activities. In particular, an increase in
122 strontium-90 (⁹⁰Sr) concentrations was observed at the SRS F Area after the reinjection of treated
123 water with high ionic strength, possibly due to the cation exchange reactions. We developed a
124 reactive transport model for strontium migration to understand the attenuation/remobilization
125 mechanism of strontium in the vicinity of the source zones. And the developed model was used to
126 investigate the difference in temporal migration behaviors of strontium and background electrolyte
127 (i.e., Na⁺, which is a proxy for ionic strength or specific conductance).

128 This strategy – although the study was conducted based on the SRS-specific data – is expected
129 to be useful for many other contaminated sites, since ⁹⁰Sr is one of the important contaminants
130 after nuclear accidents and nuclear waste operations (e.g., Chornobyl,¹⁸ Fukushima,¹⁹ and the
131 Sellafield site²⁰). The developed strategy could also be applicable at sites where ion exchange acts
132 as the predominant sorption mechanism and at contaminated sites in the coastal area, where
133 seawater intrusion could increase salinity and change geochemical conditions. Since specific
134 conductance is one of the most commonly available *in-situ* sensors, we aim to increase the use of
135 *in-situ* specific conductance sensors for an early warning application.

136 **2. METHODOLOGY**
137 **2.1. Study Site Description**
138 **2.1.1. Site Background**
139 The SRS F Area hosted a chemical processing facility for plutonium extraction using the
140 PUREX process, operated between the 1950s and 1980s in South Carolina, United States.^{21, 22} In
141 order to dispose of the low-level radioactive acidic liquid waste, three unlined seepage basins were
142 constructed at SRS F Area, and the basins received nearly 7×10^9 L of the waste solutions from
143 1955 through 1988.^{8, 21} The waste solutions contained various radionuclides (e.g., 3 H, 90 Sr, 129 I,
144 $^{137\&139}$ Cs, $^{141\&144}$ Ce, $^{235\&238}$ U, $^{238\&239}$ Pu, and 241 Am) as well as non-radiological contaminants
145 including Cr, As, Cd, Hg, and Pb.

146 Since the discharge of the waste to the basins was terminated in 1988, several remediation
147 strategies have been deployed at the site. Remediation began in 1990 with the chemical
148 stabilization of contaminated soils at the bottom of the basins and the installation of a low-
149 permeability cap at the top of the basins to limit infiltration.^{8, 9} In addition, a pump-treat-reinjection
150 system, which targeted removing radionuclides and metallic elements, was implemented in 1997.
151 The purpose of the system was to intercept and extract contaminated groundwater downstream
152 from the basins and then treat most of the contaminants (except tritium) using ion exchange,
153 reverse osmosis, and precipitation/flocculation. The treated water would then be reinjected at the
154 upstream of the basins.²¹

155 After a few years of the operation, the pump-treat-reinjection system was replaced by enhanced
156 natural attenuation using a hybrid funnel-and-gate system, in 2004.^{8, 9} This system consists of
157 multiple subsurface low-permeable barriers which are emplaced across the groundwater flow paths,
158 directing the contaminant plume into gates that are gaps between the barriers (Figure 1). Through
159 the gates, alkaline solutions are periodically injected into the groundwater to elevate the pH and
160 therefore to enhance the sequestration of radionuclides. The current ENA is expected to be
161 eventually replaced with MNA which is a promising closure strategy for the SRS.



162
 163 **Figure 1. Schematic site description of the SRS F-Area. The circles shown in the figure represent the**
 164 **monitoring wells (FSB 91D, FSB 93D, and FSB 95DR) investigated in this study.**

165 2.1.2. Monitoring of Contaminant Migration at SRS

166 Monitoring of radioactive constituents started in 1955 at the beginning of the basins' operation.
 167 Over the years, various types and number of wells, seepline monitoring points, and surface water
 168 locations have been installed at the SRS F-Area. Currently, more than 100 groundwater and surface
 169 water monitoring stations are in operation.²³ On one hand, the periodic groundwater sampling for
 170 monitoring nonradioactive contaminants began in 1982.^{8, 24} Monitoring activities for the SRS F-
 171 Area have revealed that around 1 km² of subsurface (groundwater) was contaminated and the
 172 acidic contaminant plume was extended to approximately 600 m downgradient from the basins.^{8,}
 173 ²⁵

174 In this study, about 30 years of monitoring data obtained from the monitoring wells near the SRS
 175 F-Area basins was used. We demonstrate the capabilities of the proposed early risk warning
 176 strategy with a subset of the F-Area data, including specific conductance and ⁹⁰Sr concentration.
 177 ⁹⁰Sr is the contaminant of concern whose remobilization was observed near the basins during the
 178 pump-treat-reinjection system operation. Specific conductance is considered to be a critical
 179 parameter for predicting the remobilization of ⁹⁰Sr since it can be used as a proxy for measuring
 180 changes in cations concentration that could cause the remobilization. Under the monitoring plan
 181 expected to be applied for SRS, specific conductance can be continuously and easily measurable
 182 using *in-situ* sensors.
 183

184

185

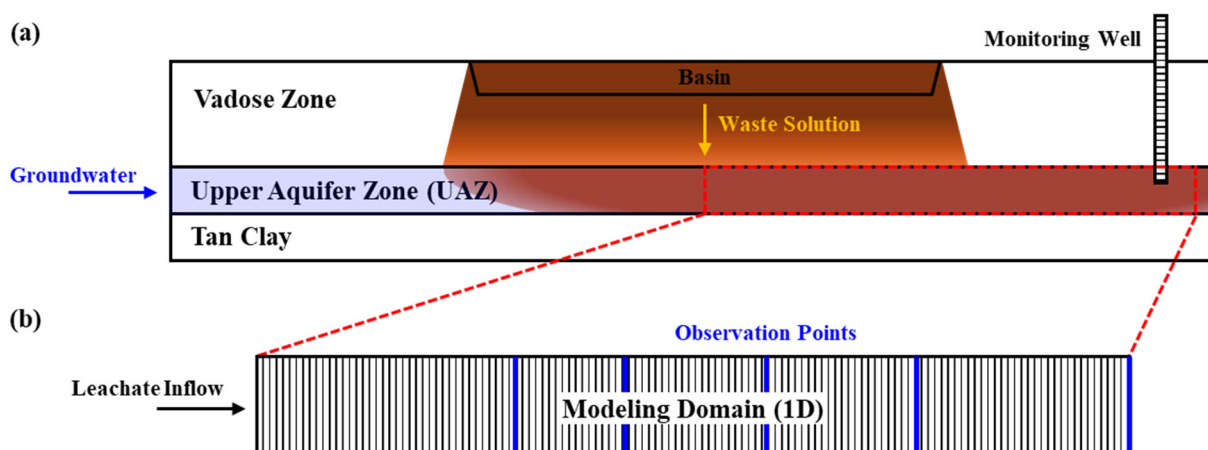
186 **2.2. Reactive Transport Modeling Approach**187 We have developed a reactive transport model using the numerical code, CrunchTope (Steefel
188 et al 2015)²⁶ to understand the attenuation and remobilization processes of strontium in the SRS
189 F-Area aquifer sediments. Briefly, this code solves the advection-dispersion equation coupled to a
190 range of geochemical reactions. Details in fundamental theories and governing equations can be
191 found in the software manual.²⁷

192

193 **2.2.1. Conceptual Model**194 The general framework of our conceptual model follows other studies for SRS, including Bea et
195 al. (2013)²⁸, Arora et al. (2018)²⁹, and Libera et al. (2019)¹⁰. As depicted in Figure 2a, previous
196 studies showed that the waste solution disposed of in the basin expected to be moved down into
197 the subsurface through the vadose zone and reached the upper aquifer zone (UAZ). The
198 contaminated plume is introduced to the UAZ through a broad area in the upper part of the UAZ
199 and could be mixed with the upstream groundwater.200 Our model uses a simplified horizontal one-dimensional (1D) domain (Figure 2b), following
201 Arora et al. (2018)²⁹. This 1D domain represents a part of the saturated UAZ beneath the F Area
202 considered as one of major contaminant plume pathways. The domain length is 227 m and
203 discretized using 227 cells with a uniform grid spacing of 1 m. Multiple observation points were
204 set in the model to understand strontium remobilization behavior according to distance between
205 monitoring wells and source zones (refer to Figure 1). Our model assumed constant Darcy velocity
206 with groundwater flowing along the horizontal axis (Figure 2).

207

208



209

210

211

Figure 2. Schematic diagram of (a) geological description of the SRS F-Area and expected plume flow in the subsurface and (b) domain of conceptual model

212

213

214

2.2.2. Hydrogeological and Geochemical Initial Conditions

215 Homogeneous hydrogeological and geochemical properties were applied to the entire domain.
216 Table 1 summarizes parameters for hydraulic and solute transport simulation used in this study.
217 The longitudinal dispersivity was calculated for the 227 m long sediment 1D column based on the
218 equation proposed by Schulze-Makuch.³⁰

219

220

Table 1. Input parameters used for hydraulic and solute transport simulation

Parameter	Value	Reference
Porosity (-)	0.39	29
Darcy flux (m/year)	48.36	21
Molecular diffusion coefficient (m ² /s)	1.80×10 ⁻⁹	29
Longitudinal dispersivity (m)	2.18	30

221

222 Table 2 summarizes the initial mineralogical composition of the sediment compiled from SRS
 223 sediment analysis report³¹ and the properties of the corresponding minerals. In the SRS report,
 224 XRD analysis was conducted for three Upper Aquifer sediment samples obtained from different
 225 depths. The analysis results showed that abundance of minerals varies with depth and major
 226 constituents were quartz, kaolinite, illite, and goethite. For simplicity, it was presumed that mineral
 227 dissolution and precipitation kinetic is very low, i.e., it was treated as like inert phases. Previous
 228 studies that considered mineral dissolution and precipitation showed that pH remained under acidic
 229 conditions.^{28, 29}

230

Table 2. Initial mineralogical composition of the 1D domain and properties of minerals considered in the simulations

Minerals	Average volume fraction	SSA (m ² /g)	CEC (meq/100g) ^d
Quartz	0.4335	0.14 ^a	1
Kaolinite	0.1044	20.6 ^b	10
Illite	0.0470	112 ^c	25
Goethite	0.0250	16.2 ^b	3

^aArora et al. (2018)²⁹; ^bDong et al. (2012)³²; ^cMacht et al. (2011)³³; ^dVerMeulen and Gonzales-Raymat (2023)³¹

233

234 Denham (2021) investigated the contributions of single mineral phases present at SFS F-Area
 235 sediments to strontium sorption, and found that silica (quartz) and goethite have small sorption
 236 capacity for strontium in acidic conditions.³⁴ In this study, therefore, the sorption of Sr to only
 237 illite and kaolinite was modeled (Table 3). We only consider cation exchange reactions without
 238 surface complexation reactions, because previous studies reported that in acidic to neutral pH
 239 conditions, the contribution of surface complexation to Sr sorption onto illite was nearly negligible
 240 compared to ion exchange.^{35, 36} In addition, isotopic effects related to strontium sorption were not
 241 considered, as they are generally regarded as insignificant and radioactive decay was not
 242 considered as well.

243

244

Table 3. Cation exchange reactions and the corresponding selectivity coefficients for illite and Kaolinite

Ion Exchange Reaction		$\log_{10}K_c$ (Illite)	$\log_{10}K_c$ (Kaolinite) ^c
Na-X	+ H ⁺ ↔ H-X	+ Na ⁺	0.0 ^a
Na-X	+ K ⁺ ↔ K-X	+ Na ⁺	1.11 ^a
2Na-X	+ Mg ²⁺ ↔ Mg-X ₂	+ 2Na ⁺	1.04 ^a
2Na-X	+ Ca ²⁺ ↔ Ca-X ₂	+ 2Na ⁺	1.04 ^a
2Na-X	+ Sr ²⁺ ↔ Sr-X ₂	+ 2Na ⁺	1.00 ^b
3Na-X	+ Al ³⁺ ↔ Al-X ₃	+ 3Na ⁺	1.00 ^a

^aBradbury and Baeyens (2009)³⁷; ^bMontoya et al. (2018)³⁵; ^cAppelo et al. (2005)³⁸

245

246

2.2.3. Simulation Sequence and the Corresponding Boundary Conditions

247

248

In order to model the abrupt changes in geochemical conditions that occurred at SRS F Area due
 to the pump-treat-reinjection remediation activities, we developed a scenario that consisted of the

249 following three sequential phases: (1) First, the 1D domain, which represents the UAZ, was
 250 preconditioned by flowing pristine groundwater for 3 years; (2) After preconditioning, seepage
 251 effluent (waste solution) was applied for 42 years. This duration reflects the period between the
 252 first disposal of acidic waste solution to the basin and the commencement of the pump-treat-
 253 reinjection system; (3) In the last phase, the domain was leached with treated water with an
 254 elevated Na^+ concentration for seven years, which corresponds to the assumed pump-treat-
 255 reinjection system operational period. Table 4 gives the chemical conditions of each solution used
 256 in the simulations. They were applied to the left boundary condition for each corresponding phase,
 257 and the right boundary condition was pristine groundwater in all phases.

258
 259 **Table 4. Chemical composition of leachates used in the simulations**

Component ($\text{mol}\cdot\text{kg}^{-1}$)	Pristine groundwater (Pre-basin-operation phase)	Seepage effluent (Contaminated water discharging phase)	Treated water (Pump-treat-reinjection system operational phase)
pH	5.40	2.05	5.40
Na^+	2.78×10^{-4}	6.82×10^{-5}	0.30
Cl^-	9.99×10^{-3}	3.39×10^{-5}	9.99×10^{-3}
$\text{CO}_2(\text{aq})$	1.22×10^{-5}	1.07×10^{-5}	1.21×10^{-5}
Al^{3+}	1.46×10^{-8}	1.00×10^{-8}	3.65×10^{-8}
Fe^{3+}	5.77×10^{-16}	5.49×10^{-6}	1.96×10^{-15}
K^+	3.32×10^{-5}	1.72×10^{-6}	3.32×10^{-5}
Ca^{2+}	1.00×10^{-5}	1.00×10^{-5}	1.00×10^{-5}
Mg^{2+}	5.35×10^{-3}	2.47×10^{-6}	5.35×10^{-3}
NO_3^-	1.00×10^{-3}	1.00×10^{-2}	3.01×10^{-1}
SO_4^{2-}	2.25×10^{-5}	4.80×10^{-5}	2.25×10^{-5}
Sr^{2+}	-	1.49×10^{-7}	-
$\text{SiO}_2(\text{aq})$	9.83×10^{-5}	1.18×10^{-4}	9.18×10^{-5}
Duration (years)	3	42	7

260

261

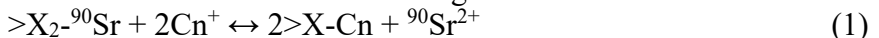
262 **3. RESULTS AND DISCUSSION**

263 **3.1. Analysis of Monitoring Data: Remobilization of ^{90}Sr Near SRS F-Area Basins**

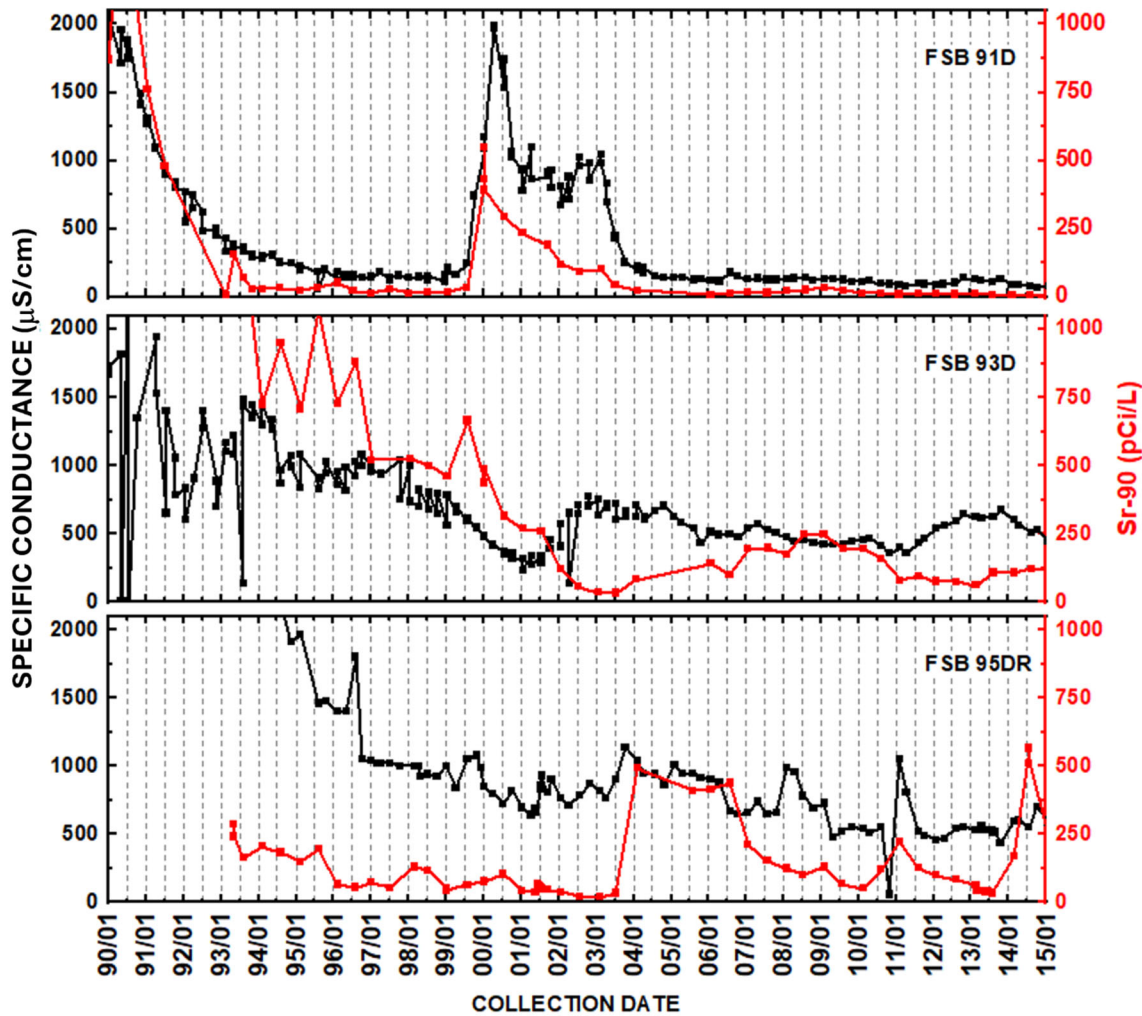
264 Specific conductance, measured at monitoring wells adjacent to the F-Area basins and located
 265 in the upper aquifer zone (UAZ), decreased after basin operations ceased but began to increase
 266 again between 1999 and 2001 (Figure 3). This increase was associated with the injection of the
 267 treated water upgradient of the basins as part of the pump-treat-reinjection system initiated in 1997.
 268 In parallel, the ^{90}Sr concentration in the wells showed a gradual decrease over time; however, it
 269 subsequently increased between 1999 and 2003. Because the increases in specific conductance and
 270 ^{90}Sr concentration occurred during the same period, these two parameters appear to be correlated.

271 One hypothesis regarding this phenomenon is that increased groundwater salinity, observed in
 272 the form of elevated specific conductance, induced the remobilization of strontium that had already
 273 been sorbed onto the sediments. This can be explained in detail in sequential phases as follows: (1)
 274 First, ^{90}Sr sorbed onto the exchangeable clays in the sediments during the contaminated plume
 275 move through the aquifer; (2) The salinity (specific conductance) of the groundwater increased, in
 276 other words, the concentration of cation increased, following the operation of pump-treat-

277 reinjection system; (3) Due to the increased concentration of the cation in the groundwater, the
 278 exchange reaction between aqueous cation and pre-adsorbed ^{90}Sr on the sediments was promoted
 279 (see Eq. 1). As a result, ^{90}Sr was remobilized and released to the groundwater.



280 where $>\text{X}$ and Cn^+ represent an exchange site on sediment and monovalent cation, respectively.
 281
 282



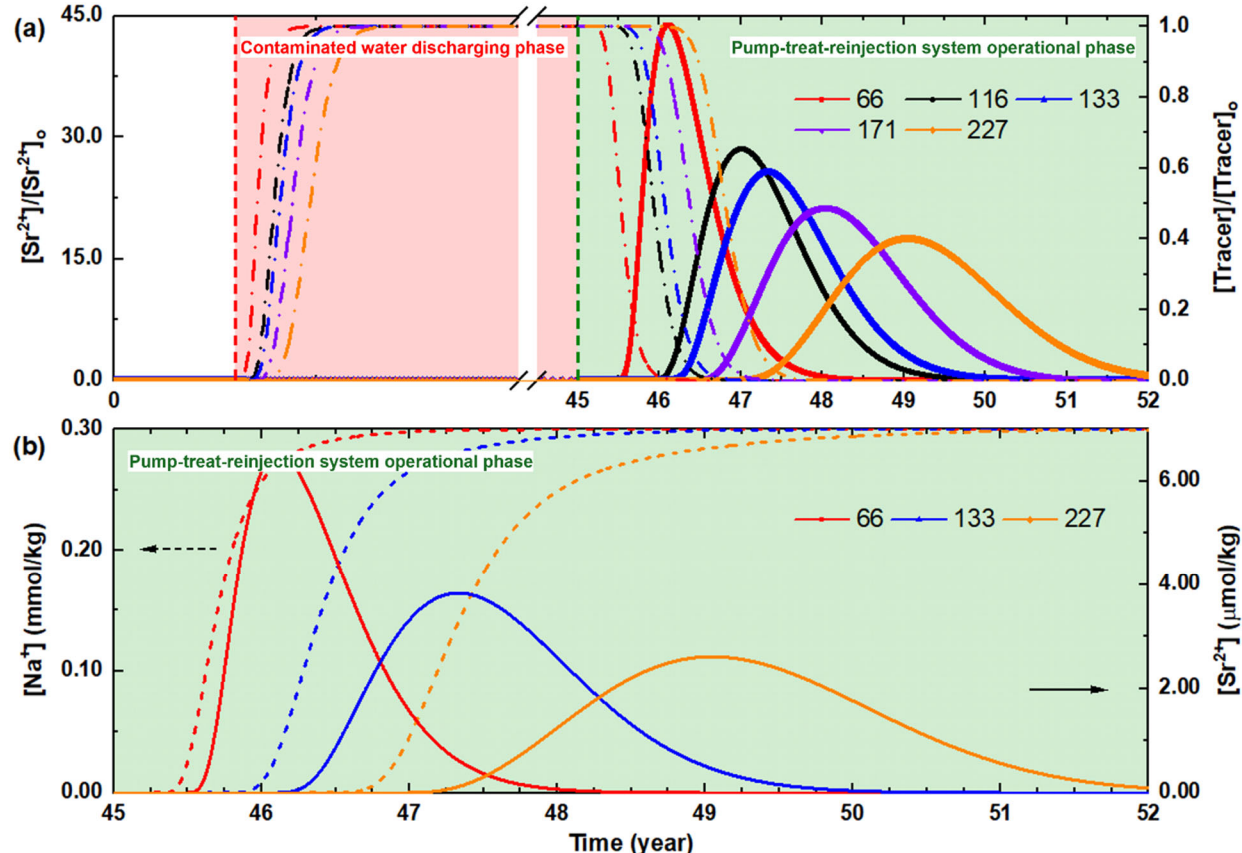
283
 284 **Figure 3. Monitoring data of specific conductance and ^{90}Sr from monitoring wells (FSB 91D, 93D, and 95DR)**
 285 located at upper aquifer zone (UAZ)

286 287 **3.2. Mechanism Behind the Remobilization of Strontium at the SRS F-Area**

288 The breakthrough curves of Sr at the multiple observation points obtained from the simulation
 289 are shown in Figure 4a. In the figure, the red area represents a phase when the contaminated water
 290 was discharged into the subsurface (the second column in Table 4). During this period, no
 291 strontium was detected at any observation points, while a non-reactive tracer was observed with a
 292 breakthrough curve, which implies that Sr sorbed onto the sediments. When the treated water
 293 (higher sodium concentration) is injected, increases in both sodium and strontium concentrations
 294 were observed at every observation point (Figure 4a and 4b). The peak Sr concentrations detected
 295 at the observation points were tens of times greater than those in the seepage effluent, which

296 implies that this Sr did not originate only from the contaminated plume. The modeling results
 297 capture the trend observed in the monitoring data from the F-Area wells (Figure 3), which supports
 298 the hypothesis that abrupt changes in ionic strength caused the ^{90}Sr remobilization by promoting
 299 an ion exchange reaction between aqueous cations and strontium originally built-up onto
 300 sediments.

301
 302



303
 304 Figure 4. Breakthrough curve of (a) Sr^{2+} (solid line) and tracer (dash-dotted line) at various observation
 305 points (left and right y-axes represent a ratio of Sr^{2+} and tracer concentration in porewater to initial Sr^{2+} and
 306 tracer concentration in seepage effluent, respectively) and (b) Na^+ (dashed line) and Sr^{2+} (solid line): shows
 307 the pump-treat-reinjection system operational period only

308

309 3.3. Early Risk Warning Strategy for Remobilization of Strontium

310 As shown in Figure 3, the increase in specific conductance was observed first, prior to the
 311 increase in ^{90}Sr concentration (FSB 93D and 95DR), and a similar trend was observed in our
 312 simulations. Regardless of observation points, an increase of Na^+ (indicative of specific
 313 conductance), was detected first after the injection of the treated water, and an increase in Sr^{2+}
 314 concentration arrived later (Figure 4b). This phenomenon is expected to be due to the fact that Na^+
 315 and Sr^{2+} have different sorption affinity onto clays. In general, Na^+ has lower sorption affinity
 316 compared to Sr^{2+} and therefore, moves faster than Sr^{2+} . Even though desorption of Sr^{2+} occurred
 317 near the upstream end of the domain due to increased Na^+ concentration, it can be sorbed onto
 318 sediment again as it moves downstream, i.e., retardation in Sr^{2+} migration can occur. For these
 319 reasons, an increase in specific conductance can be detected prior to increase in ^{90}Sr concentration.

320 The lag between changes in specific conductance and strontium concentration depends on the path
321 length of the contaminant plume. As can be seen from Figure 4b, the time difference between
322 increase in Na^+ concentration and Sr^{2+} concentration becomes more apparent downstream.
323 Consistent trends are also seen in the monitoring data when comparing FSB 91D and FSB 93D
324 data in Figure 3 (refer to Figure 1 for comparing the locations of the wells).

325 Based on this difference in temporal behavior of specific conductance and strontium, specific
326 conductance could be used as an indicator of remobilization of ^{90}Sr . For example, if a sudden
327 increase in specific conductance was detected, then one can expect there might be an increase in
328 ^{90}Sr in the near future. During that period, additional remediation can be applied to the site to
329 mitigate the expected remobilization. Furthermore, if the lag between such indicators (e.g., specific
330 conductance) and contaminant migration is understood sufficiently, even the extent and occurrence
331 time of the contaminant remobilization would be predictable.

332

333 **3.4. Sensitivity Analysis: The Effect of Cation Concentration and Flow Rate on** 334 **Remobilization of Strontium**

335 To understand how the degree of change in specific conductance affects the remobilization
336 characteristics of strontium, sensitivity analysis was conducted. Three different types of treated
337 water with different sodium ion concentrations (0.25 mol/kg, 0.3 mol/kg, and 0.4 mol/kg) were
338 used in the simulations. As shown in Figure 5a, the remobilization of strontium is significantly
339 affected by the sodium concentration in the treated water. Higher sodium concentrations were
340 associated with a higher and narrower Sr^{2+} peak, implying that a higher cation concentration causes
341 more intensive remobilization.

342 In addition, this analysis shows the time lag between the *in-situ* measurable parameters and
343 contaminant concentration depends not only on the observation locations but also on the sodium
344 concentrations. A shorter time difference between Na^+ and Sr^{2+} concentration increase was
345 observed with higher sodium concentration. The simulation results also showed that changing
346 groundwater velocity has a similar effect. We compared the temporal behavior of Sr^{2+}
347 remobilization with different groundwater velocity (Figure 5b). If the groundwater velocity
348 increased, accelerated remobilization was observed with an increased and narrowed Sr^{2+} peak, and
349 the opposite phenomenon was observed when it decreased. Consistent with these observations, the
350 time difference between Na^+ and Sr^{2+} concentration increase becomes intensified with a reduced
351 groundwater velocity.

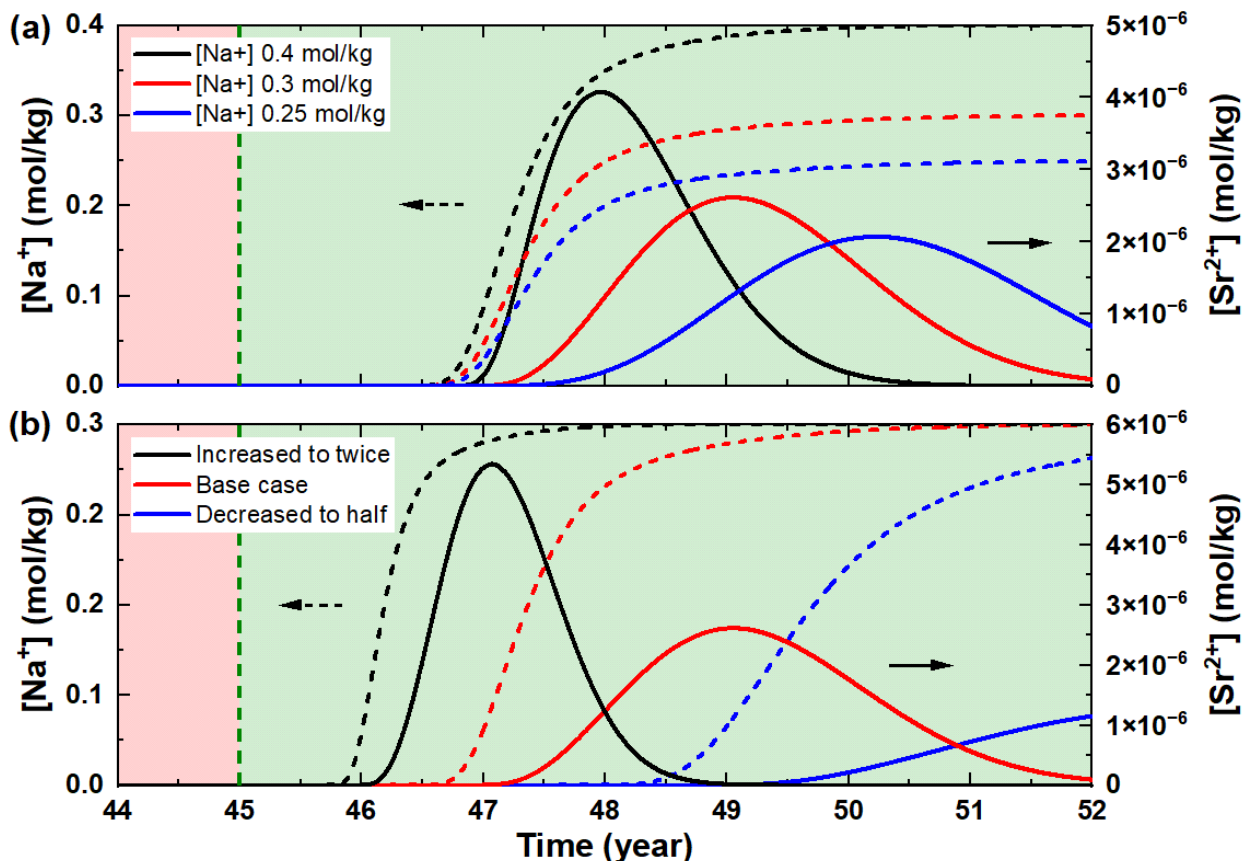


Figure 5. Sensitivity analysis for analyzing the effect of (a) cation (Na^+) concentration and (b) groundwater velocity on the temporal behavior of Sr remobilization. Dash line and solid line represent changes in Na^+ and Sr^{2+} concentration, respectively. The red and green shaded areas in the figures indicate the contaminated water discharging phase and the pump-treat-reinjection system operational phase, respectively.

4. CONCLUSION

In the present study, a reactive transport model was developed to understand the migration characteristics of the contaminant in the subsurface under abrupt changes in geochemical conditions, and to identify the mechanism of ^{90}Sr remobilization observed at the SRS F Area during the operation of the pump-treat-reinjection system. The historical monitoring data from the SRS F Area and our reactive transport modeling results showed that there was a time lag between the migration of a background electrolyte and the remobilized contaminant under abrupt changes in geochemical conditions. In particular, an increase in specific conductance (or Na^+ concentration) was detected first at the monitoring wells before a remobilized contaminant arrived at the well. These findings suggest that the remobilization of contaminants, mainly attenuated through an ion exchange reaction, induced by abrupt changes in geochemical conditions can be predicted by monitoring the specific conductance of the groundwater, which is real-time and readily measurable using *in-situ* sensors.

Our findings also show how changes in the environmental conditions affect the effectiveness of the proposed strategy. For example, the time lag between the migration of a background electrolyte

375 and the remobilized contaminant, and the peak concentration of the contaminant varied with
376 background cation concentration and groundwater velocity.

377 We acknowledge the limitations in our study. Because the model employed a simplified one-
378 dimensional (1D) column domain, it may not fully account for variations in water elevation, which
379 could also influence the behavior of ⁹⁰Sr. This study aimed at improving our system understanding
380 rather than quantitatively matching the observation data. In addition, due to limited data availability,
381 the model assumed the chemical composition of the leachates and injected solutions such as
382 sodium concentrations. We addressed such uncertainty using the sensitivity analysis. This
383 modeling approach serves an important step toward the long-term management of contaminated
384 sites where the ion exchange reaction is mostly responsible for the attenuation of the contaminants
385 (e.g., low pH soil contaminated by Pb and Cd³⁹) by providing the means to detect the
386 remobilization of contaminants before the remobilization occurs.

387

388 **CRedit authorship contribution statement**

389 **Sol-Chan Han:** Conceptualization, Formal analysis, Investigation, Methodology, Visualization,
390 Writing – original draft. **Hansell Gonzalez-Raymat:** Data curation, Investigation, Resources,
391 Visualization, Writing – review and editing. **Miles Denham:** Investigation, Validation, Writing –
392 review and editing. **Toshiyuki Bandai:** Methodology, Software, Writing – review and editing.
393 **Zexuan Xu:** Formal analysis, Methodology, Supervision. **Sergi Molins:** Formal analysis,
394 Investigation, Methodology, Project administration, Supervision, Writing – review and editing.
395 **Haruko Wainwright:** Conceptualization, Formal analysis, Funding acquisition, Investigation,
396 Methodology, Project administration, Supervision, Writing – original draft

397

398 **Declaration of Competing Interest**

399 The authors declare no competing financial interest.

400

401 **ACKNOWLEDGMENT**

402 This research was supported by ALTEMIS (Advanced Long-term Environmental Monitoring
403 Systems), supported by the U.S. Department of Energy Office of Environmental Management.

404

405 **REFERENCES**

- 406 (1) Cao, T.; Liu, Y.; Gao, C.; Yuan, Y.; Chen, W.; Zhang, T. Understanding Nanoscale
407 Interactions between Minerals and Microbes: Opportunities for Green Remediation of
408 Contaminated Sites. *Environ Sci Technol* **2024**, *58* (32), 14078-14087. DOI:
409 10.1021/acs.est.4c05324.
- 410 (2) Singh, B. K.; Naidu, R. Cleaning contaminated environment: a growing challenge.
411 *Biodegradation* **2012**, *23* (6), 785-786. DOI: 10.1007/s10532-012-9590-5.
- 412 (3) Hou, D.; Al-Tabbaa, A.; O'Connor, D.; Hu, Q.; Zhu, Y.-G.; Wang, L.; Kirkwood, N.; Ok, Y.
413 S.; Tsang, D. C. W.; Bolan, N. S.; et al. Sustainable remediation and redevelopment of
414 brownfield sites. *Nature Reviews Earth & Environment* **2023**, *4* (4), 271-286. DOI:
415 10.1038/s43017-023-00404-1.

416 (4) Naidu, R. Recent Advances in Contaminated Site Remediation. *Water, Air, & Soil Pollution*
417 **2013**, 224 (12), 1705. DOI: 10.1007/s11270-013-1705-z.

418 (5) *Superfund: National Priorities List (NPL)*. United States Environmental Protection Agency
419 (USEPA), <https://www.epa.gov/superfund/superfund-national-priorities-list-npl> (accessed
420 October 15, 2024).

421 (6) Wilson, K.; Sewell, G.; Kean, J. A.; Vangelas, K. Enhanced attenuation: Its place in the
422 remediation of chlorinated solvents. *Remediation Journal* **2007**, 17 (2), 39-49. DOI:
423 <https://doi.org/10.1002/rem.20123>.

424 (7) Yong, R. N.; Mulligan, C. N. *Natural and enhanced attenuation of contaminants in soils*;
425 CRC Press, 2019.

426 (8) Schmidt, F.; Wainwright, H. M.; Faybisenko, B.; Denham, M.; Eddy-Dilek, C. In Situ
427 Monitoring of Groundwater Contamination Using the Kalman Filter. *Environ Sci Technol* **2018**,
428 52 (13), 7418-7425. DOI: 10.1021/acs.est.8b00017.

429 (9) Denham, M. E.; Amidon, M. B.; Wainwright, H. M.; Dafflon, B.; Ajo-Franklin, J.; Eddy-
430 Dilek, C. A. Improving Long-term Monitoring of Contaminated Groundwater at Sites where
431 Attenuation-based Remedies are Deployed. *Environmental Management* **2020**, 66 (6), 1142-
432 1161. DOI: 10.1007/s00267-020-01376-4.

433 (10) Libera, A.; de Barros, F. P. J.; Faybisenko, B.; Eddy-Dilek, C.; Denham, M.; Lipnikov, K.;
434 Moulton, D.; Maco, B.; Wainwright, H. Climate change impact on residual contaminants under
435 sustainable remediation. *Journal of Contaminant Hydrology* **2019**, 226, 103518. DOI:
436 <https://doi.org/10.1016/j.jconhyd.2019.103518>.

437 (11) Cavelan, A.; Golfier, F.; Colombano, S.; Davarzani, H.; Deparis, J.; Faure, P. A critical
438 review of the influence of groundwater level fluctuations and temperature on LNAPL
439 contaminations in the context of climate change. *Science of The Total Environment* **2022**, 806,
440 150412. DOI: <https://doi.org/10.1016/j.scitotenv.2021.150412>.

441 (12) Crawford, S. E.; Brinkmann, M.; Ouellet, J. D.; Lehmkuhl, F.; Reicherter, K.;
442 Schwarzbauer, J.; Bellanova, P.; Letmathe, P.; Blank, L. M.; Weber, R.; et al. Remobilization of
443 pollutants during extreme flood events poses severe risks to human and environmental health.
444 *Journal of Hazardous Materials* **2022**, 421, 126691. DOI:
445 <https://doi.org/10.1016/j.jhazmat.2021.126691>.

446 (13) Xu, Z.; Serata, R.; Wainwright, H.; Denham, M.; Molins, S.; Gonzalez-Raymat, H.;
447 Lipnikov, K.; Moulton, J. D.; Eddy-Dilek, C. Reactive transport modeling for supporting climate
448 resilience at groundwater contamination sites. *Hydrology and Earth System Sciences* **2022**, 26
449 (3), 755-773. DOI: 10.5194/hess-26-755-2022.

450 (14) Hill, K.; Hirschfeld, D.; Lindquist, C.; Cook, F.; Warner, S. Rising Coastal Groundwater as
451 a Result of Sea-Level Rise Will Influence Contaminated Coastal Sites and Underground
452 Infrastructure. *Earth's Future* **2023**, 11 (9), e2023EF003825. DOI:
453 <https://doi.org/10.1029/2023EF003825>.

454 (15) Declercq, I.; Cappuyns, V.; Duclos, Y. Monitored natural attenuation (MNA) of
455 contaminated soils: State of the art in Europe—A critical evaluation. *Science of The Total
456 Environment* **2012**, 426, 393-405. DOI: <https://doi.org/10.1016/j.scitotenv.2012.03.040>.

457 (16) Meray, A. O.; Sturla, S.; Siddiquee, M. R.; Serata, R.; Uhlemann, S.; Gonzalez-Raymat, H.;
458 Denham, M.; Upadhyay, H.; Lagos, L. E.; Eddy-Dilek, C.; et al. PyLEnM: A Machine Learning
459 Framework for Long-Term Groundwater Contamination Monitoring Strategies. *Environ Sci
460 Technol* **2022**, 56 (9), 5973-5983. DOI: 10.1021/acs.est.1c07440.

461 (17) Siddiquee, M. R.; Meray, A. O.; Xu, Z.; Gonzalez-Raymat, H.; Danielson, T.; Upadhyay,
462 H.; Lagos, L. E.; Eddy-Dilek, C.; Wainwright, H. M. Machine Learning Approach for
463 Spatiotemporal Multivariate Optimization of Environmental Monitoring Sensor Locations.
464 *Artificial Intelligence for the Earth Systems* **2024**, 3 (4), e230011. DOI:
465 <https://doi.org/10.1175/AIES-D-23-0011.1>.

466 (18) Igarashi, Y.; Protsak, V.; Laptev, G.; Maloshtan, I.; Samoilov, D.; Kirieiev, S.; Onda, Y.;
467 Konoplev, A. Effects of Large-Scale Wildfires on the Redistribution of Radionuclides in the
468 Chornobyl River System. *Environ Sci Technol* **2024**, 58 (46), 20630-20641. DOI:
469 10.1021/acs.est.4c07019.

470 (19) Castrillejo, M.; Casacuberta, N.; Breier, C. F.; Pike, S. M.; Masqué, P.; Buesseler, K. O.
471 Reassessment of 90Sr, 137Cs, and 134Cs in the Coast off Japan Derived from the Fukushima
472 Dai-ichi Nuclear Accident. *Environ Sci Technol* **2016**, 50 (1), 173-180. DOI:
473 10.1021/acs.est.5b03903.

474 (20) Thorpe, C. L.; Law, G. T. W.; Lloyd, J. R.; Williams, H. A.; Atherton, N.; Morris, K.
475 Quantifying Technetium and Strontium Bioremediation Potential in Flowing Sediment Columns.
476 *Environ Sci Technol* **2017**, 51 (21), 12104-12113. DOI: 10.1021/acs.est.7b02652.

477 (21) Wan, J.; Tokunaga, T. K.; Dong, W.; Denham, M. E.; Hubbard, S. S. Persistent Source
478 Influences on the Trailing Edge of a Groundwater Plume, and Natural Attenuation Timeframes:
479 The F-Area Savannah River Site. *Environ Sci Technol* **2012**, 46 (8), 4490-4497. DOI:
480 10.1021/es204265q.

481 (22) Zhang, S.; Ho, Y.-F.; Creeley, D.; Roberts, K. A.; Xu, C.; Li, H.-P.; Schwehr, K. A.;
482 Kaplan, D. I.; Yeager, C. M.; Santschi, P. H. Temporal Variation of Iodine Concentration and
483 Speciation (127I and 129I) in Wetland Groundwater from the Savannah River Site, USA.
484 *Environ Sci Technol* **2014**, 48 (19), 11218-11226. DOI: 10.1021/es502003q.

485 (23) Danielson, T. L. *Sensor Recommendations for Long Term Monitoring of the F-Area
486 Seepage Basins*; SRNL-STI-2020-00208; Savannah River National Laboratory, United States,
487 2020. DOI: 10.2172/1643940.

488 (24) Killian, T. H.; Kolb, N. L.; Corbo, P.; Marine, I. W. *Environmental Information Document
489 F-Area Seepage Basins*; DPST-85-706; Savannah River Laboratory, 1987.

490 (25) Denham, M. E.; Eddy-Dilek, C. A.; Wainwright, H. M.; Thibault, J.; Boerstler, K. *A New
491 Paradigm for Long Term Monitoring at the F-Area Seepage Basins, Savannah River Site*;
492 SRNL-STI-2019-00019; Savannah River National Laboratory, United States, 2019. DOI:
493 10.2172/1504623.

494 (26) Steefel, C. I.; Yabusaki, S. B.; Mayer, K. U. Reactive transport benchmarks for subsurface
495 environmental simulation. *Computational Geosciences* **2015**, 19 (3), 439-443. DOI:
496 10.1007/s10596-015-9499-2.

497 (27) Steefel, C. I. *CrunchFlow*; 2015.

498 (28) Bea, S. A.; Wainwright, H.; Spycher, N.; Faybishenko, B.; Hubbard, S. S.; Denham, M. E.
499 Identifying key controls on the behavior of an acidic-U(VI) plume in the Savannah River Site
500 using reactive transport modeling. *Journal of Contaminant Hydrology* **2013**, 151, 34-54. DOI:
501 <https://doi.org/10.1016/j.jconhyd.2013.04.005>.

502 (29) Arora, B.; Davis, J. A.; Spycher, N. F.; Dong, W.; Wainwright, H. M. Comparison of
503 Electrostatic and Non-Electrostatic Models for U(VI) Sorption on Aquifer Sediments.
504 *Groundwater* **2018**, 56 (1), 73-86. DOI: <https://doi.org/10.1111/gwat.12551>.

505 (30) Schulze-Makuch, D. Longitudinal dispersivity data and implications for scaling behavior.
506 *Groundwater* **2005**, 43 (3), 443-456. DOI: <https://doi.org/10.1111/j.1745-6584.2005.0051.x>.

507 (31) VerMeulen, H. H.; Gonzales-Raymat, H. *Cation Exchange Capacity, Anion Exchange*
508 *Capacity, and Mineralogy of F-Area Aquifer Sediments*; SRNL-STI-2023-00481; Savannah
509 River National Laboratory, United States, 2023. DOI: 10.2172/2202352.

510 (32) Dong, W.; Tokunaga, T. K.; Davis, J. A.; Wan, J. Uranium(VI) Adsorption and Surface
511 Complexation Modeling onto Background Sediments from the F-Area Savannah River Site.
512 *Environ Sci Technol* **2012**, *46* (3), 1565-1571. DOI: 10.1021/es2036256.

513 (33) Macht, F.; Eusterhues, K.; Pronk, G. J.; Totsche, K. U. Specific surface area of clay
514 minerals: Comparison between atomic force microscopy measurements and bulk-gas (N2) and -
515 liquid (EGME) adsorption methods. *Applied Clay Science* **2011**, *53* (1), 20-26. DOI:
516 <https://doi.org/10.1016/j.clay.2011.04.006>.

517 (34) Denham, M. E. *Conceptual Model of Sr-90 Behavior in Groundwater of the F- and H-Area*
518 *Seepage Basins, Savannah River Site: Potential Attenuation Mechanism*; PanEnv-2021-002;
519 Panoramic Environmental Consulting, LLC, 2021.

520 (35) Montoya, V.; Baeyens, B.; Glaus, M. A.; Kupcik, T.; Marques Fernandes, M.; Van Laer, L.;
521 Bruggeman, C.; Maes, N.; Schäfer, T. Sorption of Sr, Co and Zn on illite: Batch experiments and
522 modelling including Co in-diffusion measurements on compacted samples. *Geochimica et*
523 *Cosmochimica Acta* **2018**, *223*, 1-20. DOI: <https://doi.org/10.1016/j.gca.2017.11.027>.

524 (36) Missana, T.; Garcia-Gutierrez, M.; Alonso, U. Sorption of strontium onto illite/smectite
525 mixed clays. *Physics and Chemistry of the Earth, Parts A/B/C* **2008**, *33*, S156-S162. DOI:
526 <https://doi.org/10.1016/j.pce.2008.10.020>.

527 (37) Bradbury, M. H.; Baeyens, B. Sorption modelling on illite Part I: Titration measurements
528 and the sorption of Ni, Co, Eu and Sn. *Geochimica et Cosmochimica Acta* **2009**, *73* (4), 990-
529 1003. DOI: <https://doi.org/10.1016/j.gca.2008.11.017>.

530 (38) Appelo, C. A. J.; Postma, D. *Geochemistry, Groundwater and Pollution*; CRC press, 2005.
531 DOI: doi.org/10.1201/9781439833544.

532 (39) Serrano, S.; O'Day, P. A.; Vlassopoulos, D.; García-González, M. T.; Garrido, F. A surface
533 complexation and ion exchange model of Pb and Cd competitive sorption on natural soils.
534 *Geochimica et Cosmochimica Acta* **2009**, *73* (3), 543-558. DOI:
535 <https://doi.org/10.1016/j.gca.2008.11.018>.

536